Electrochimica Acta 129 (2014) 276–282

Contents lists available at ScienceDirect

Electrochimica Acta

journal homepage: www.elsevier.com/locate/electacta

# Photovoltaic performance improvement of dye-sensitized solar cells through introducing In-doped $TiO_2$ film at conducting glass and mesoporous $TiO_2$ interface as an efficient compact layer

Xiaohua Sun[a,*], Qiaoling Zhang[a], Yumin Liu[b], Niu Huang[a], Panpan Sun[a], Tao Peng[b], Tianyou Peng[b,1], Xing-Zhong Zhao[b,2]

[a] College of Materials and Chemical Engineering, Collaborative Innovation Center for Energy Equipment of Three Gorges Region, China Three Gorges University, Yichang 443002, China
[b] School of Physics and Technology, College of Chemistry and Molecular Science, Wuhan University, Wuhan 430072, China

ARTICLE INFO

*Article history:*
Received 7 November 2013
Received in revised form 20 February 2014
Accepted 20 February 2014
Available online 7 March 2014

*Keywords:*
In-doped titania
Compact layer
Dye sensitized solar cells

ABSTRACT

In-doped $TiO_2$ thin film was introduced at the interface of fluorine-doped tin oxide (FTO) substrate and mesoporous $TiO_2$ film by spin-coating method, and its application as a new compact layer material for dye-sensitized solar cells (DSSCs) was investigated. The scanning electron microscopy (SEM), UV-visible spectroscopy, current-voltage characteristics, Mott-Schottky analysis, electrochemical impedance spectroscopy (EIS) analysis and open-circuit voltage decay (OCVD) technique are used to characterize the morphology, optical transmittance and flat-band potentials ($V_{fb}$) of In-doped titania compact film and its effect to the photoelectron conversion process. It was found that In-doping increased the transmittance of $TiO_2$ compact layer, the interfacial resistance between FTO substrate and porous $TiO_2$ film and the flat-band potential of $TiO_2$ film. The In-doped $TiO_2$ compact layer effectively suppressed the charge recombination from FTO to the electrolyte, increased the optical absorption of dye and then increased the short-circuit photocurrent density ($J_{sc}$). Furthermore, In-doped $TiO_2$ compact layer acted as a weak energy barrier, which increased the electron density in the mesoporous $TiO_2$ film, thus improved open-circuit photovoltage ($V_{oc}$). As a result, the overall energy conversion efficiency of the DSSC with In-doped $TiO_2$ compact layer was enhanced by 11.9% and 6.9% compared to the DSSC without compact layer and with pure $TiO_2$ compact layer, respectively. It indicated that In-doped $TiO_2$ is a promising compact layer material for dye-sensitized solar cells.



## 1. Introduction

Dye-sensitized solar cell (DSSC) consists of a dye adsorbed mesoporous $TiO_2$ layer on fluorine-doped tin oxide (FTO) glass as a photo-electrode, a Pt counter electrode and an electrolyte normally containing $I^-/I_3^-$ redox couple [1–5]. It has drawn much attention during last two decades because it has been regarded as an environmentally friendly and low-cost solar energy conversion device [6,7]. There are four important interfaces in DSSC: FTO/porous $TiO_2$, porous $TiO_2$/dye, dye/electrolyte, and electrolyte/counter electrode. At these interfaces, photogenerated electrons may recombine with the oxidized species (such as $I_3^-$ in the redox electrolyte or dye cations) [8], which caused the photocurrent loss and seriously decrease the photovoltaic performance of DSSC [9,10]. Recently, some researchers have employed considerable strategies to modify these interfaces to improve the performance of the device. A well-known method is modifying the porous $TiO_2$/dye interface through introducing metal oxides such as $Nb_2O_5$ [11,12], ZnO [13,14], MgO [15,16], $Al_2O_3$ [17], CdO [18], or Carbonates $CaCO_3$ [19,20], $BaCO_3$ [21], etc. to form an energy barrier between the $TiO_2$ nanoparticles and the dye or electrolyte. It allows electron injection but hinders the recombination reaction. In addition, a few efforts have been made to modify the FTO/porous $TiO_2$ interface to optimize the performance of DSSCs by employing a compact layer [10,22–24]. However, researches on such important interface is not intense as compared to modification of the others [25].

It was argued that recombination in DSSC occurs predominantly near the transparent conducting oxide (TCO) substrate supporting

* Corresponding author. Tel.: +86 717 6397560; fax: +86 717 6397559.
*E-mail addresses:* mksxh@163.com (X. Sun), typeng@whu.edu.cn (T. Peng), xzzhao@whu.edu.cn (X.-Z. Zhao).
[1] Tel.: +86 27 87642784; fax: +86 27 87642569.
[2] Tel.: +86 27 8721 8474; fax: +86 27 6875 4067.

http://dx.doi.org/10.1016/j.electacta.2014.02.110
0013-4686/

the titania film, as opposed to homogeneously throughout the film from the intensity-modulated infrared transmittance measurements [26]. It was also reported that retarding the recombination at the TCO/electrolyte interface was very important especially for solid state DSSCs, quantum dot, and organic dye sensitized solar cells [23]. Even for new hybrid solar cells based on meso-superstructured organometal halide perovskites, a compact layer was also coated on the FTO glass to reduce charge recombination for obtaining high photoelectric conversion efficiency (10.9%) [27]. So it is vital to introduce an effective compact layer onto the FTO glass to block the electron recombination. Usually, a dense $TiO_2$ thin film prepared with an organic sol dip-coating method [10] or $TiCl_4$ aqueous solution soaking method [28] was employed as compact layer to obstruct the back electron transfer from the FTO to the electrolyte; Recently, some wide band-gap oxides, such as ZnO [25] and $Nb_2O_5$ [29], have been used as a blocking layer. They suppressed charge recombination and dark current effectively, thus improved open-circuit photovoltage ($V_{oc}$) and fill factor (FF), however, depressed the short-circuit current ($J_{sc}$) for its very high potential barrier. In addition, Nb donor doped $TiO_2$ thin film was deposited on FTO substrate to form a compact film by pulsed laser deposition (PLD), which achieved better photovoltage performance than the DSSC with pure $TiO_2$ compact layer [30]. Nevertheless, the PLD method is not the best choice for industrialization due to the high manufacture cost and small deposition area.

As far as we know, up to present, few groups investigated the acceptor doped $TiO_2$ thin film modifying the FTO/prous $TiO_2$ interface and its effect on the performance of DSSCs. In this study, In acceptor doped $TiO_2$ thin film was introduced at the interface of FTO substrate and mesoporous $TiO_2$ film as a compact blocking layer by spin-coating method. The influence of In doping on some physical characterizations of $TiO_2$ compact layer and photoelectron conversion process are characterized and discussed.

## 2. Experimental

### 2.1. Chemicals.

Tetrabutyl titanate (TBT), diethanol amine, polyethylene glycol (PEG, MW = 20,000), Triton X-100, absolute ethanol (99.7%), indium nitrate ($In(NO_3)_3{\cdot}4.5H_2O$), concentrated nitric acid ($HNO_3$, 65%∼68%), glacial acetic acid ($CH_3COOH$, ≥99.5%) and propylene carbonate (PC) were purchased from Sinopharm Chemical Reagent Co.Ltd (China). Iodine ($I_2$, 99.8%) was purchased from Beijing Yili chemicals (China). Lithium iodide (LiI, 99%), titanium tetraisopropoxide (TTIP, Ti-($OC_3H_7$), 98%), and 4-tert-butylpyr-idine (TBP) were obtained from Acros. The Ru dye, cis-di(thiocyanato)-bis(2,2′-bipyridyl-4,4′-dicarboxylate) ruthenium(II) (N719), was purchased from Solaronix (Switzer-land). All the reagents used were of analytical purity. Fluorine-doped $SnO_2$ conductive glass (FTO, sheet resistance $10-15\ \Omega\ sq^{-1}$) purchased from Asahi Glass (Japan) was used as the substrate for the deposition of a mesoporous nanocrystalline $TiO_2$ film.

### 2.2. Preparation of In-doped titania films on FTO substrates and photoelectrodes.

Pure and 6 mol % In-doped titania films on FTO substrates were prepared using the sol–gel method. $In(NO_3)_3{\cdot}4.5H_2O$ was dissolved in absolute ethanol, followed by adding diethanol amine under vigorous stirring for 5 min. Then TBT was added to the above solution with constant stirring for 10 min. The final concentration of TBT was adjusted to 0.26 M through adding the right amount of absolute ethanol. The solutions were mixed and stirred at 60 °C for 30 min to obtain clear solution. The pure and 6 mol % In-doped titania precursor solution was coated on the FTO substrates at 2600 rpm for 30 sec by the spin-coating method. The as-deposited titania films on FTO substrates were annealed at 550 °C for 30 min in a muffle furnace to obtain pure $TiO_2$ and 6 mol % In-doped $TiO_2$ compact layer. The corresponding samples were labeled as FTO/PTO and FTO/ITO, respectively.

A nanocrystalline $TiO_2$ paste for fabricating the mesoporous nanocrystalline $TiO_2$ layer of electrode was prepared according to the reported procedure. [31] The prepared $TiO_2$ paste was coated on the bare FTO, FTO/PTO and FTO/ITO substrates by a doctor blade method. After drying under the infrared lamp, the films were calcined at 500 °C for 30 min in a muffle furnace to obtain photoelectrodes.

### 2.3. DSSC fabrication.

The photoelectrodes washed by the absolute ethanol were preheated at 110 °C for 30 min. Then the photoelectrodes were immersed in absolute ethanol containing 0.5 mM Ru-dye $(Bu_4N)_2[Ru\text{-}(Hdcbpy)_2(NCS)_2]$ (N719 dye, Solaronix) at 60 °C for 12 h. The dye-sensitized $TiO_2$ electrodes were rinsed with absolute ethanol and dried at 70 °C for 30 min in an oven. A sandwich-type DSSC were fabricated by clipping the N719 dye-sensitized $TiO_2$ photoelectrode and a platinized FTO counter electrode and then introducing electrolyte between the electrodes. The electrolyte solution was composed of 0.1 M 1-propyl-3-methylimidazolium iodide (PMII), 0.05 M LiI, 0.1 M guanidinium thiocyanate (GNCS), 0.03 M $I_2$, and 0.5 M 4- tert-butylpridine (TBP) in a mixed solvent of acetonitrile and propylene carbonate (PC) (volume ratio: 1/1).

### 2.4. Characterization.

The surface and cross-sectional morphologies of the FTO, FTO/PTO and FTO/ITO substrates were observed by using a high-resolution field emission scanning electron microscopy (SEM, Sirion FEG, USA). The optical transmittance spectra of the FTO, FTO/PTO and FTO/ITO substrates were measured using a UV-vis spectrophotometer (Cary 5000, Varian). In order to determine the flat band potentials of $TiO_2$ and In-doped $TiO_2$ films, Mott-Schottky plots were obtained in a three-electrode cell containing one of these films as the working electrode, a platinum plate as the counter electrode and a saturated Ag/AgCl electrode as the reference electrode. The entire area of the photoanode, except the active area (1 $cm^2$), was blocked using an adhesive tape. The electrolyte solution was composed of 10 mM LiI, 1 mM $I_2$, and 0.1 M $LiClO_4$ in acetonitrile was used as the electrolyte. The electrochemical impedance spectra were recorded by a PC-controlled CHI660 C electrochemical workstation applying a sinusoidal perturbation of 5 mV at a frequency of 100 Hz and a cell voltage from -1.2 to -0.2 V with a scan rate of 5 mV/step towards the anodic direction. Photocurrent–voltage characteristics (J–V curves) were measured employing a solar light simulator (Oriel 91192, USA) at 100 $mWcm^{-2}$ (AM 1.5, global) which was calibrated by a Si-1787 Photodiode and a computer-controlled CHI660 C electrochemical workstation. The irradiated area of each cell was kept at 0.25 $cm^2$ by using a light-tight metal mask for all samples. The open-circuit voltage decay (OCVD) was recorded by turning off the illumination on DSSC in a steady state and monitoring the subsequent decay of Voc. Electrochemical impedance spectroscopy (EIS) was carried out under open-circuit potential condition and 100 $mWcm^{-2}$ bias illumination. The frequency range was 0.05∼100000 Hz and the magnitude of modulation signal was 0.01 V. The above measurements were carried out on the CHI660 C electrochemical workstation combined with Xenon light source.

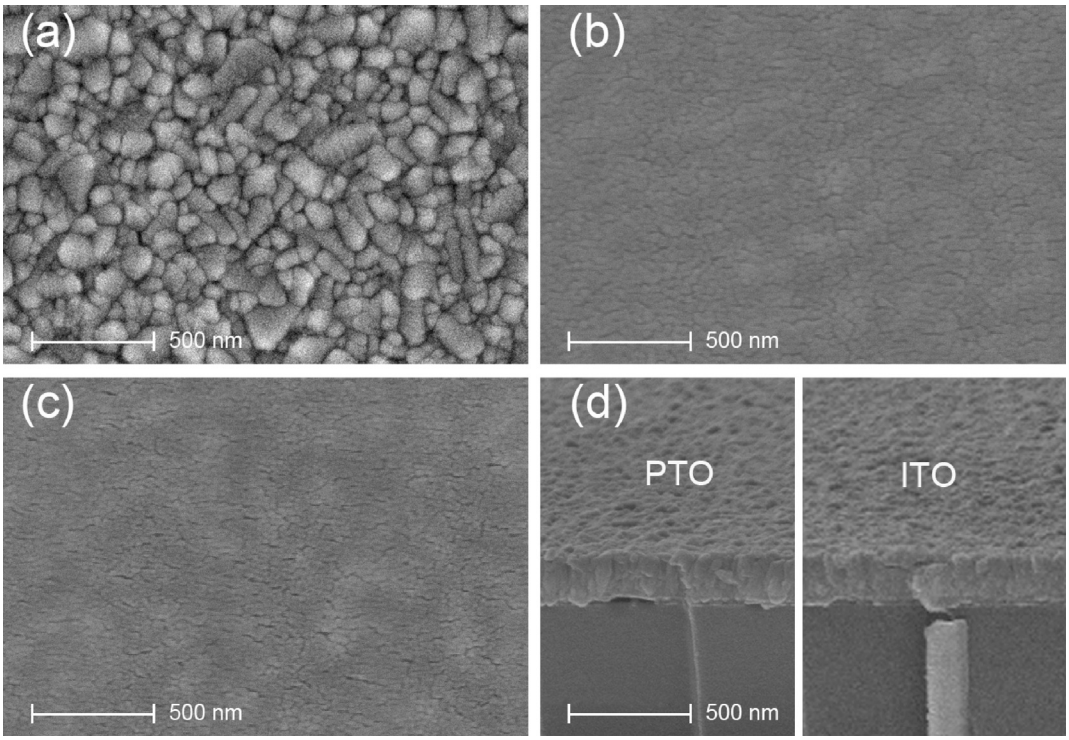


**Fig. 1.** SEM surface morphologies of (a) FTO, (b) pure and (c) 6% In-doped $TiO_2$ compact films, (d) cross-sectional SEM image of FTO/PTO and FTO/ITO substrates.

## 3. Results and discussion

### 3.1. Characterization of different substrates.

Fig. 1 shows the SEM surface morphologies of FTO, FTO/PTO and FTO/ITO substrates and the cross-sectional SEM image of FTO/PTO and FTO/ITO substrates, respectively. The bare FTO surface shows the characteristic morphology of F doped tin oxide crystals (Fig. 1 a), whose grain size is around 80∼150 nm and surface is relative rough. After $TiO_2$ films are coated on FTO substrates, the morphologies of FTO disappear. Pure and 6 mol % In-doped $TiO_2$ films show smooth and dense surface morphologies and the In-doped $TiO_2$ film shows smaller grain size (about 30∼50 nm) than the pure $TiO_2$ film. The thickness of the pure and 6 mol % In-doped $TiO_2$ film is very close and is about 200 nm (as shown in Fig. 1 d). The thickness of compact layer may play an important role in performance of DSSC, which will be further studied in the future.

Since DSSCs are illuminated from the FTO substrate side in working conditions, it is necessary for us to investigate the optical properties of the substrates after introducing the compact blocking layers. Fig. 2 shows the UV-vis transmission spectra of the bare FTO, FTO/PTO and FTO/ITO substrates. It is obvious that the transmittances of the multilayered substrates are both lower than that of the bare FTO in all wavelength regions. But the transmittances of FTO/PTO and FTO/ITO substrates are both not lower than 75% at 550 nm, which is considered to be high enough to be employed in DSSCs [30]. Compared with the FTO/PTO, the transmittance of the FTO/ITO slightly increases at 380∼470 nm, which may be related to its smaller grain sizes (as shown in Fig. 1. b and c). According to Mie theory, the particle with small grain size (< 200 nm) usually shows low light scattering ability [32]. So the transmittance of ITO coating should increases for its smaller grain sizes. Furthermore, the thin film with small grain usually has low surface roughness [33,34]. The decrease of surface roughness causes the decrease in reflection and optical absorption [35], and thus the transmittance of the film also increases. The higher transmittance of the FTO/ITO may promote the optical absorption of dye loading on nanocrystalline titanium dioxide and then improve the short-circuit photocurrent density ($J_{sc}$).

### 3.2. Determination of flat-band potential.

The flat-band potential ($E_{fb}$) of the electrode material in a DSSC is very important because the quasi-Fermi level of the semiconductor oxide photoelectrode ($TiO_2$) increases linearly with $E_{fb}$ [36,37]. To confirm the effect of In doping on the flat-band potentials of $TiO_2$ compact layers, the Mott-Schottky plots of the pure $TiO_2$ and In-doped $TiO_2$ films were performed at a frequency of 100 Hz at room temperature (as shown in Fig. 3). In the Mott-Schottky analysis, a linear relationship is predicted between the inverse square of the capacitance ($1/C^2$) and applied potential, arising from the semiconductor space charge layer in depletion under the biasing conditions

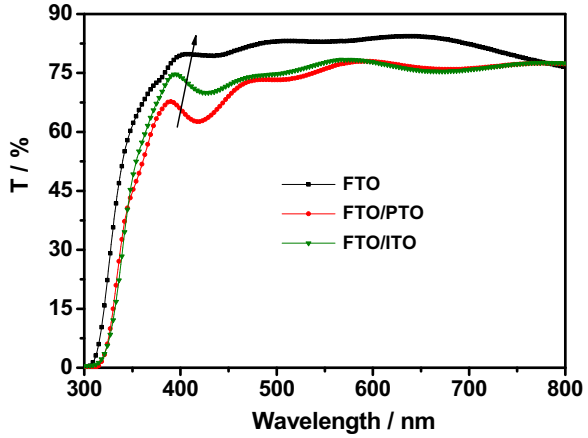


**Fig. 2.** UV-vis transmittances of bare FTO, FTO/PTO and FTO/ITO substrates.

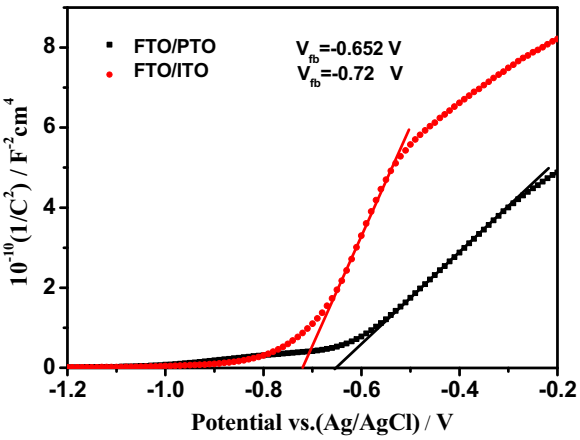


**Fig. 3.** Mott-Schottky plots of FTO/PTO and FTO/ITO substrates.

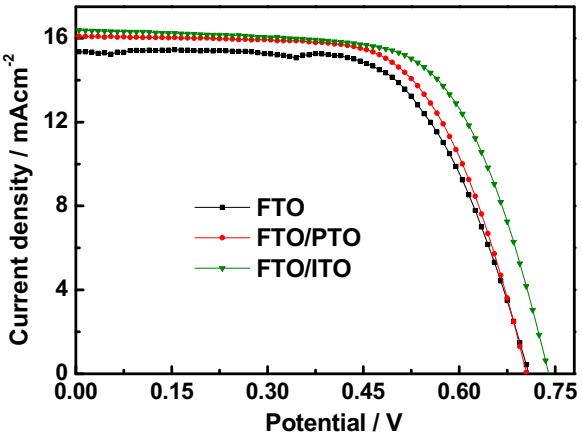


**Fig. 4.** Photocurrent density-voltage (J-V) curves of DSSCs based on bare FTO, FTO/PTO and FTO/ITO substrates at AM 1.5 irradiation of 100 mW/cm$^2$.

[37]. The capacitance of the space charge region can be described as follows [38,39]:

$$1/C_{SC}^2 = \frac{2(E - E_{fb} - kT/e)}{e\varepsilon\varepsilon_0 N_D}$$

Where $C_{sc}$ is the space charge capacity, $\varepsilon$ is the dielectric constant of the $TiO_2$ films, $\varepsilon_0$ is the dielectric constant of vacuum, $e$ is the electronic charge, $N_D$ is the charge carrier density, $E$ is the applied potential, $k$ is the Boltzmann constant, $T$ is the absolute temperature.

Fig. 3 shows Mott-schottky plots of the pure $TiO_2$ and In-doped $TiO_2$ films. Fitting the linear part of the Mott-schottky plots and extrapolating the fitting lines to C = 0, the flat band potential $E_{fb}$ can be determined. The calculated $E_{fb}$ for the pure $TiO_2$ and 6% In-doped $TiO_2$ compact layers is -0.652 and -0.720 $V$ (vs. Ag/AgCl), respectively. Compared with the pure $TiO_2$ compact layer, the $E_{fb}$ of the 6% In-doped $TiO_2$ compact layer shifted negatively about 0.068 $V$, which suggests that quasi-Fermi level of the In-doped $TiO_2$ compact layer is higher than that of the pure $TiO_2$ compact layer. That is to say, In-doped $TiO_2$ compact layer creates a potential barrier between FTO substrate and porous $TiO_2$ film, which can block the electron injection from the conduction band of porous $TiO_2$ to FTO, further increase the electron density in porous $TiO_2$ film and then enhance its quasi-Fermi level. In DSSCs, open-circuit voltage ($V_{oc}$) is determined by the difference between the redox potential of the electrolyte and the quasi-Fermi level of the semiconductor oxide photoelectrode [40]. Therefore, the rise of the quasi-Fermi level of porous $TiO_2$ caused by In-doped $TiO_2$ compact layer with higher flat-band potential will improve the $V_{oc}$.

### 3.3. Photovoltaic performance of DSSCs.

Fig. 4 shows the photocurrent density-voltage (*J-V*) curves of DSSCs based on bare FTO, FTO/PTO and FTO/ITO substrates at AM 1.5 irradiation of 100 mAcm$^{-2}$. The photoelectric conversion parameters of DSSCs based on different substrates are summarized in Table 1. The $J_{sc}$, $V_{oc}$ and fill factor (*FF*) of the DSSC based on bare FTO substrate are 15.348 mAcm$^{-2}$, 0.705 V and 0.63, respectively, corresponding to an energy conversion efficiency of 7.01%. After introducing pure and In-doped $TiO_2$ compact layers on FTO substrates, the devices gave some different degrees of improvements in $J_{sc}$, $V_{oc}$ and *FF*. Especially in the case of the DSSC based on FTO/ITO substrate, the $J_{sc}$, $V_{oc}$ and *FF* increases 6.75% (from 15.348 to 16.384 mAcm$^{-2}$), 4.26% (from 0.705 V to 0.735 V) and 4.9% (from 0.63 to 0.661), respectively. As a result, the device shows the highest energy conversion efficiency ($\eta$) of 7.96%. It is 14% higher than that of the DSSC based on FTO substrate ($\eta$ = 7.01%). Compared to the DSSC with pure $TiO_2$ compact layer, the DSSC with 6% In-doped $TiO_2$ compact layer gives higher $J_{sc}$, $V_{oc}$ and *FF*, and then higher energy conversion efficiency ($\eta$). Higher $J_{sc}$ may be ascribed to the In-doped $TiO_2$ compact layer more effectively suppressing back electron transfer from FTO to electrolyte (as shown in Fig. 5), prolonging the electron lifetime (as shown in Fig. 7 and Fig. 9) and improving the light absorption (as shown in Fig. 2). At the same time, the formation of effective $TiO_2$ blocking layer on the FTO reduces the shunt current, which improves the fill factor [41].

**Table 1**
Photovoltaic performance data of DSSCs Based on different electrodes.

| Sample | Jsc (mA·cm$^{-2}$) | $V_{oc}$ (V) | FF | η (%) |
|---|---|---|---|---|
| FTO | 15.348 | 0.705 | 0.63 | 7.01 |
| FTO/PTO | 16.084 | 0.705 | 0.653 | 7.41 |
| FTO/ITO | 16.384 | 0.735 | 0.661 | 7.96 |

The dark current is not a good simulation of the recombination current under illumination. However, it can be used as an estimate of the extent of reduction of $I_3^-$ with electrons. To investigate the effect of different compact layers on suppressing back electron transfer from FTO to electrolyte, the dark currents for the DSSCs are also measured and are shown in Fig. 5. It can be seen that, after introducing pure and In-doped $TiO_2$ compact layer on FTO substrates, the dark current of DSSC decreases. Especially for the DSSC with 6% In-doped $TiO_2$ compact layer, the dark current decreases markedly and the onset potential of the dark current shifts to higher

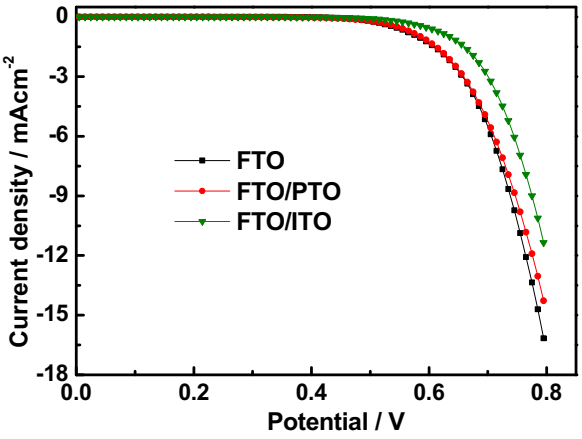


**Fig. 5.** J-V curves of DSSCs based on bare FTO, FTO/PTO and FTO/ITO substrates measured in the dark.

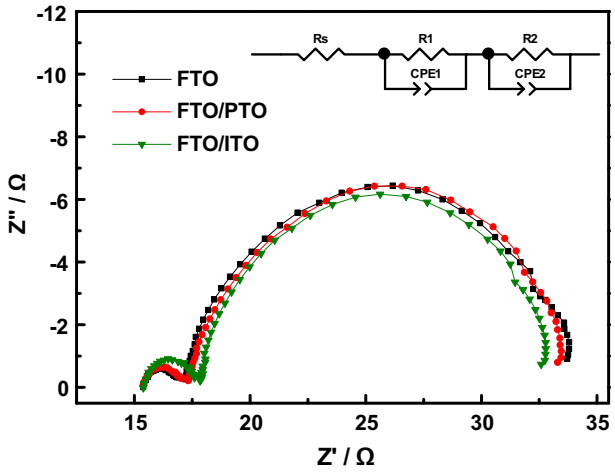


**Fig. 6.** Nyquist plots of the DSSCs employing the bare FTO, FTO/PTO and FTO/ITO substrates.

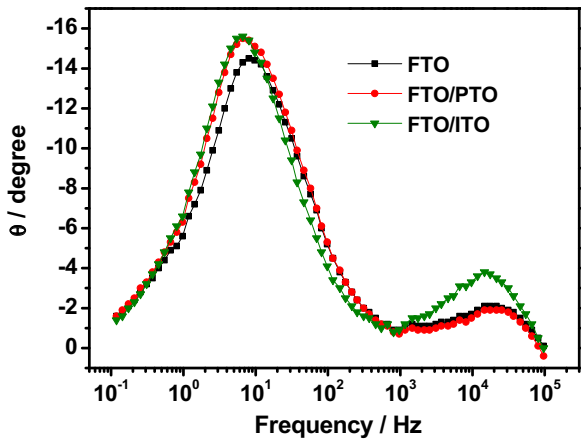


**Fig. 7.** Bode phase plots of the DSSCs based on bare FTO, FTO/PTO and FTO/ITO substrates.

voltage (from 0.42 *V* to 0.45 *V*). It demonstrates that the In-doped $TiO_2$ compact layer successfully suppresses the charge recombination between electrons emanating from the FTO substrate and $I_3^-$ ions presented in the electrolyte and In-doped $TiO_2$ is a good compact layer material in DSSCs.

### 3.4. Electrochemical impedance spectra analyses.

Electrochemical impedance spectroscopy (EIS) analysis has been regarded as a useful tool for investigating the electron transport and recombination in DSSCs. To better understand dynamics of electron transport and reveal the difference in the interfacial characteristics of the DSSCs based on different substrates, the electrochemical impedance spectroscopy of DSSCs under one-sun illumination was measured ranging from 0.1 *Hz* to 100 *kHz* at the $V_{oc}$. Fig. 6 shows the Nyquist plots of the DSSCs based on different substrates. In all the EIS spectra, two semicircles were observed in the high-frequency region (>1 *kHz*) and in the frequency region of 100∼1 *Hz*, respectively. According to the EIS model reported in the literature [42–44], the smaller semicircle in the high-frequency region represents the charge transport at the FTO/$TiO_2$ and Pt/electrolyte interfaces, and the larger one denotes the charge transfer at the $TiO_2$/dye/electrolyte interface. Table 2 summarizes the results of the EIS analysis fitted by using an equivalent circuit containing constant phase element (CPE) and resistance (*R*) shown in the inset of Fig. 6.

The value of $R_1$ is the sum of resistances of counter electrode/electrolyte and FTO/$TiO_2$ interfaces [45]. Since an identical Pt counter electrode was employed for all the devices, the change of $R_1$ is ascribed to the noticeable difference at the interfaces of FTO/$TiO_2$. It can be seen from the Table 2 that the value of $R_1$ for three devices based on FTO, FTO/PTO and FTO/ITO substrates increases gradually, which implies that the pure and the In-doped $TiO_2$ compact layers increase the interfacial resistance between FTO substrate and porous $TiO_2$ film and the In-doping can efficiently increase the value of $R_1$. Furthermore, the change trend of $R_1$ for these three devices is consistent with the variation tendency of dark current (as shown in Fig. 5) and electron lifetime (as shown in Fig. 7 and Fig. 9) for these three devices. It discloses the capability of different compact layers constraining the electrons on FTO electrode coming back and decreasing the charge recombination.

In addition, $R_2$, the charge-transfer resistance at the $TiO_2$/dye/electrolyte interface, decreases for devices with high interfacial resistance $R_1$, which may be related to the high electron density in the conductive band of porous $TiO_2$ film [46,47]. For the In-doped $TiO_2$ compact layer with high interfacial resistance $R_1$ and flat-band potential ($E_{fb}$), it creates an energy barrier at the interface of FTO/$TiO_2$ and blocks the electrons injecting from the conduction band of porous $TiO_2$ to FTO. As a consequence, the photogenerated electrons will accumulate in the conduction band of porous $TiO_2$, which leads to the increase of electron density in the conductive band of porous $TiO_2$.

As shown in Fig. 7, the bode phase plots of EIS spectra display the frequency peaks of the charge transfer process at different interfaces for three kinds of solar anodes. The electron lifetime ($\tau_e$) in DSSCs is inversely proportional to the characteristic frequency ($f_{max}$) of the maximum phase shift in the mid-frequency peak [48]. As can be seen in Table 2, the characteristic frequencies ($f_{max}$) at the mid-frequency peaks are 9.766, 8.071 and 6.643 *Hz* for FTO, FTO/PTO and FTO/ITO devices, respectively. An increased trend of $\tau_e$ in a sequence of FTO < FTO/PTO < FTO/ITO cells is concluded, which indicates that In-doped $TiO_2$ compact layer efficiently improves the electron lifetime of DSSCs.

**Table 2**
EIS parameters of DSSCs determined by fitting the experimental data according to the equivalent circuit model (as shown in Fig.7).

| Sample | $R_1$ (Ω) | $R_2$ (Ω) | $f_{max}$ (Hz) |
|---|---|---|---|
| FTO | 1.511 | 17.26 | 9.766 |
| FTO/PTO | 1.854 | 16.82 | 8.071 |
| FTO/PTO | 2.187 | 15.56 | 6.643 |

### 3.5. Open-circuit voltage decay (OCVD) measurement.

The open-circuit voltage decay (OCVD) technology has been widely used to investigate the interfacial recombination process between the injected electrons in $TiO_2$ and the electrolyte under open-circuit and dark state in a photochemical cell [49,50]. whereas the recombination process between the injected electrons and the oxidized dye molecules cannot be measured by the OCVD [51]. In order to understand the effect of various substrates on the electron lifetime and explore the origin of the increase in electron lifetime of DSSC with In-doped $TiO_2$ compact layer, OCVD characteristics of these three devices were measured. Fig. 8 illustrates representative voltage decay curves of three devices. And the electron lifetimes (recombination response time, $\tau_n'$) for these devices

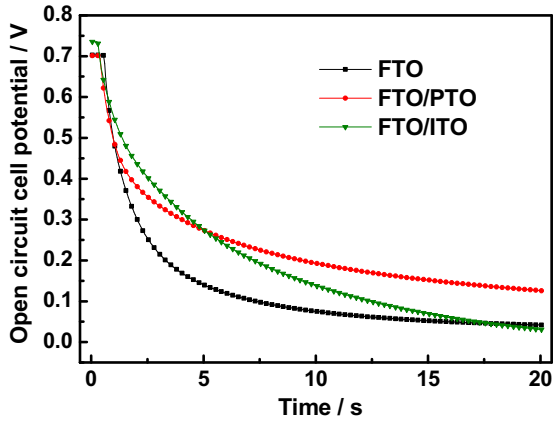


**Fig. 8.** Open-circuit voltage decay plots of the DSSCs employing the bare FTO, FTO/PTO and FTO/ITO substrates.

under open-circuit condition are calculated from the decay curve of the photovoltage by the following equation:

$$\tau_n' = \frac{k_B T}{e}\left(\frac{dV_{OC}}{dt}\right)^{-1}$$

where $k_BT$ is the thermal energy and $e$ is the positive elementary charge. The electron lifetime as a function of $V_{oc}$ $(V)$ was plotted in Fig. 9.

It can be seen from Fig. 9 that the electron lifetime for devices based on FTO, FTO/PTO and FTO/ITO substrates increases stepwise in the high $V_{oc}$ region (> 0.6 $V$), which is consistent with the results of EIS analyses and is also in a good agreement with the variation tendency of resistance $R_1$ for corresponding these devices. The electron lifetime in the high photovoltage region can closely reflect the status of the charge recombination between electrons in photoanodes and oxidized electrolyte ($I_3^-$) under illumination. The electrons involved in the charge recombination derive from the following two parts: (1) the dye-loaded porous $TiO_2$ film and (2) the FTO electrode. Because there are bulk traps and surface states in the porous $TiO_2$ film. The injected electrons in the porous $TiO_2$ film are firstly trapped by these defect states and then relaxed [51], which delays the recombination speed of electrons in the porous $TiO_2$ film with the oxidized electrolyte and then prolongs the electron lifetime. However, electrons in FTO electrode which is in direct contact with the electrolyte will immediately recombine with the oxidized species in the electrolyte. So the recombination speed of electrons in the latter with the oxidized electrolyte is faster than that in the former, and then the electron lifetime in the latter is also shorter than that in the former. Therefore, for two parts of electrons involved in the charge recombination, if the recombination reaction of the electrons on FTO with the oxidized species dominates, the electron lifetime of the device should be short; And if the charge recombination reaction of the electrons in FTO with the oxidized species is restrained, the electron lifetime of the device should become longer. Since the porous $TiO_2$ films were prepared with the identical fabrication procedures, the defect states inside the porous $TiO_2$ film for each sample should be uniform. Under the premise of the same electron density in porous $TiO_2$ films, charge recombination processes of the electrons inside the porous $TiO_2$ film with the oxidized species also should be the same. For the two DSSCs with compact layers, the $TiO_2$ compact layer prevents electrons in FTO electrode from contacting with the oxidized species efficiently, and restrains efficiently the recombination reaction of the electrons in FTO with the oxidized species. Therefore, electron lifetime of these two DSSCs is larger than that of DSSC base on the bare FTO substrate. Furthermore, the electron lifetime for DSSCs based on FTO/PTO and FTO/ITO substrates should increase stepwise for corresponding higher $R_1$ interface resistance.

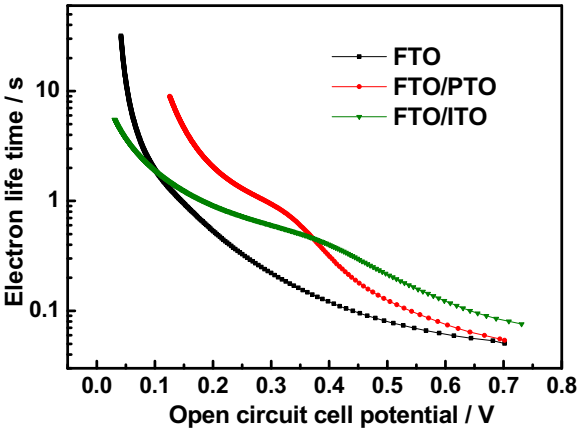


**Fig. 9.** Electron lifetime as a function of the open-circuit voltage of DSSCs based on the bare FTO, FTO/PTO and FTO/ITO substrates.

In fact, the electron density in porous $TiO_2$ film on FTO/ITO substrate would increase to some extent for In-doped $TiO_2$ compact layer with higher potential barrier blocking the electrons injection from the conductive band of porous $TiO_2$ to FTO. According to the viewpoint of Y.M. Liu [25], higher electron density would further increase the charge recombination between electrons in porous $TiO_2$ film and oxidized electrolyte ($I_3^-$) and then decrease the electron lifetime. However, in this work, the electron lifetime of DSSCs with In-doped $TiO_2$ compact layers is not lower than that of DSSC base on the bare FTO substrate. It might be because the effect of In-doped $TiO_2$ compact layer increasing the lifetime of electrons on FTO substrate is stronger than that of decreasing the lifetime of electrons in porous $TiO_2$ film. So the electron lifetime and current density of DSSC with In-doped $TiO_2$ compact layer both increased, unlike the DSSC with ZnO compact layer whose electron lifetime and current density both decreased for the high potential barrier of ZnO compact layer [25]. It indicates that the In-doped $TiO_2$ film is a kind of more excellent compact layer for DSSCs.

## 4. Conclusions

In summary, pure and In-doped $TiO_2$ thin films were fabricated on FTO substrates as compact blocking layers by spin-coating method. The influence of In-doping on the surface morphology, UV-vis transmittances, flat-band potential of $TiO_2$ compact layer was characterized. Furthermore, we discussed its effect on the photoelectron conversion process by current-voltage characteristics, electrochemical impedance spectroscopy (EIS) analysis and open-circuit voltage decay (OCVD) technique. It was found that In-doping increased the transmittance and the flat-band potential of the $TiO_2$ film, effectively suppressed the back electron transfer, thus improved open-circuit photovoltage ($V_{oc}$) and short-circuit photocurrent density ($J_{sc}$) due to its effect of blocking layer and weak energy barrier. Finally, the DSSC with 6% In-doped $TiO_2$ compact layer achieved the highest energy conversion efficiency (7.96%), which was 11.9% higher than that of DSSC without compact layer and 6.9% higher than that of DSSC with pure $TiO_2$ compact layer. It indicated that In-doped $TiO_2$ is a promising compact layer material for dye-sensitized solar cells.

## Acknowledgements

This work was supported by the National Natural Science Foundation of China under Grant No. 50902085.

## References


[1] B. Lee, D.-K. Hwang, P. Guo, S.-T. Ho, D.B. Buchholtz, C.-Y. Wang, R.P.H. Chang, J Phys Chem B 114 (2010) 14582–14591.
[2] J. Yu, Q. Li, Z. Shu, Electrochim Acta 56 (2011) 6293–6298.
[3] S.-H. Han, S. Lee, H. Shin, H. Suk Jung, Advanced Energy Materials 1 (2011) 546–550.
[4] F.d.r. Sauvage, J.-D. Decoppet, M. Zhang, S.M. Zakeeruddin, P. Comte, M. Nazeeruddin, P. Wang, M. Grätzel, J Am Chem Soc 133 (2011) 9304–9310.
[5] I.K. Ding, N. Tétreault, J. Brillet, B.E. Hardin, E.H. Smith, S.J. Rosenthal, F. Sauvage, M. Grätzel, M.D. McGehee, Adv Funct Mater 19 (2009) 2431–2436.
[6] M. Wu, X. Lin, Y. Wang, L. Wang, W. Guo, D. Qi, X. Peng, A. Hagfeldt, M. Gratzel, T. Ma, J Am Chem Soc 134 (2012) 3419–3428.
[7] H.S. Jung, J.-K. Lee, The Journal of Physical Chemistry Letters 4 (2013) 1682–1693.
[8] C. Zhang, S. Chen, H. Tian, Y. Huang, Z. Huo, S. Dai, F. Kong, Y. Sui, J Phys Chem B 115 (2011) 8653–8657.
[9] Z.-S. Wang, M. Yanagida, K. Sayama, H. Sugihara, Chem Mater 18 (2006) 2912–2916.
[10] H. Yu, S.Q. Zhang, H.J. Zhao, G. Will, P.R. Liu, Electrochim Acta 54 (2009) 1319–1324.
[11] E. Barea, X. Xu, V. Gonzalez-Pedro, T. Ripolles-Sanchis, F. Fabregat-Santiago, J., Bisquert, Energy & Environmental Science (2011).
[12] S. Chen, S. Chappel, Y. Diamant, A. Zaban, Chem. Mater, 13 (2001) 4629–4634.
[13] Z.S. Wang, C.H. Huang, Y.Y. Huang, Y.J. Hou, P.H. Xie, B.W. Zhang, H.M. Cheng, Chem Mater 13 (2001) 678–682.
[14] S.S. Kim, J.H. Yum, Y.E. Sung, J Photoch Photobio A 171 (2005) 269–273.
[15] H. Jung, J. Lee, M. Nastasi, S. Lee, J. Kim, J. Park, K. Hong, H. Shin, Langmuir 21 (2005) 10332–10335.
[16] SujuanWu, H. Han, Q. Tai, J. Zhang, S. Xu, C. Zhou, Y. Yang, H. Hu, B. Chen, B. Sebo, X.-Z. Zhao, Nanotechnology 19 (2008) 215704.
[17] B. O'Regan, S. Scully, A. Mayer, E. Palomares, J. Durrant, J Phys Chem B 109 (2005) 4616–4623.
[18] M.H. Kim, Y.U. Kwon, J Phys Chem B 113 (2009) 17176–17182.
[19] N. Okada, S. Karuppuchamy, M. Kurihara, Chem Lett 34 (2005) 16–17.
[20] S. Lee, J.Y. Kim, S.H. Youn, M. Park, K.S. Hong, H.S. Jung, J.-K. Lee, H. Shin, Langmuir 23 (2007) 11907–11910.
[21] X. Wu, L. Wang, F. Luo, B. Ma, C. Zhan, Y. Qiu, J Phys Chem B 111 (2007) 8075–8079.
[22] S. Ito, P. Liska, P. Comte, R.L. Charvet, P. Pechy, U. Bach, L. Schmidt-Mende, S.M. Zakeeruddin, A. Kay, M.K. Nazeeruddin, M. Gratzel, Chem Commun (2005) 4351–4353.
[23] A. Burke, S. Ito, H. Snaith, U. Bach, J. Kwiatkowski, M. Gr tzel, Nano Letters 8 (2008) 977–981.
[24] J.H. Noh, S. Lee, J.Y. Kim, J.-K. Lee, H.S. Han, C.M. Cho, I.S. Cho, H.S. Jung, K.S. Hong, J Phys Chem B 113 (2009) 1083–1087.
[25] Y. Liu, X. Sun, Q. Tai, H. Hu, B. Chen, N. Huang, B. Sebo, X.-z. Zhao, J Power Sources 196 (2011) 475–481.
[26] K. Zhu, E.A. Schiff, N.-G. Park, J.v.d. Lagemaat, A.J. Frank, Appl Phys Lett 80 (2002) 685–687.
[27] H.S. Kim, C.R. Lee, J.H. Im, K.B. Lee, T. Moehl, A. Marchioro, S.J. Moon, R. Humphry-Baker, J.H. Yum, J.E. Moser, M. Gratzel, N.G. Park, Sci Rep 2 (2012) 591.
[28] J.F. Shi, J. Liang, S.J. Peng, W. Xu, J. Pei, J. Chen, Solid State Sci 11 (2009) 433–438.
[29] J. Xia, N. Masaki, K. Jiang, Y. Wada, S. Yanagida, Chem Lett 35 (2006) 252–253.
[30] S. Lee, J.H. Noh, H.S. Han, D.K. Yim, D.H. Kim, J.-K. Lee, J.Y. Kim, H.S. Jung, K.S. Hong, J Phys Chem B 113 (2009) 6878–6882.
[31] S. Ito, T.N. Murakami, P. Comte, P. Liska, C. Gratzel, M.K. Nazeeruddin, M. Gratzel, Thin Solid Films 516 (2008) 4613–4619.
[32] W.E. Vargas, G.A. Niklasson, Sol Energ Mat Sol C 69 (2001) 147–163.
[33] X. Sun, B. Zhu, T. Liu, M. Li, X.-Z. Zhao, D. Wang, C. Sun, H.L.W. Chan, J Appl Phys 99 (2006) 084103–084106.
[34] X. Sun, S. Guo, G. Wu, M. Li, X. Zhao, J Cryst Growth 290 (2006) 121–126.
[35] B.L. Zhu, J. Wang, S.J. Zhu, J. Wu, D.W. Zeng, C.S. Xie, Thin Solid Films 520 (2012) 6963–6969.
[36] M. Radecka, M. Wierzbicka, S. Komornicki, M. Rekas, Physica B-Condensed Matter 348 (2004) 160–168.
[37] J. Bandara, U.W. Pradeep, Thin Solid Films 517 (2008) 952–956.
[38] J. Liu, H. Yang, W. Tan, X. Zhou, Y. Lin, Electrochim Acta 56 (2010) 396–400.
[39] M. Radecka, M. Rekas, A. Trenczek-Zajac, K. Zakrzewska, J Power Sources 181 (2008) 46–55.
[40] S.M. Yang, H.Z. Kou, S.L. Song, H.J. Wang, W.H. Fu, Colloid Surface A 340 (2009) 182–186.
[41] B. Liu, E.S. Aydil, Journal of American Chemical Society 131 (2009) 3985–3990.
[42] M. Adachi, M. Sakamoto, J.T. Jiu, Y. Ogata, S. Isoda, J Phys Chem B 110 (2006) 13872–13880.
[43] F. Fabregat-Santiago, J. Bisquert, E. Palomares, L. Otero, D.B. Kuang, S.M. Zakeeruddin, M. Gratzel, J Phys Chem B 111 (2007) 6550–6560.
[44] Q. Wang, S. Ito, M. Grätzel, F. Fabregat-Santiago, I. Mora-Seró, J. Bisquert, T. Bessho, H. Imai, J Phys Chem B 110 (2006) 25210–25221.
[45] T. Hoshikawa, R. Kikuchi, K. Eguchi, J Electroanal Chem 588 (2006) 59–67.
[46] F. Fabregat-Santiago, J. Bisquert, G. Garcia-Belmonte, G. Boschloo, A. Hagfeldt, Sol Energ Mat Sol C 87 (2005) 117–131.
[47] X. Sun, Y. Liu, Q. Tai, B. Chen, T. Peng, N. Huang, S. Xu, T. Peng, X.-Z. Zhao, J Phys Chem B 116 (2012) 11859–11866.
[48] H.S. Jung, J.-K. Lee, S. Lee, K.S. Hong, H. Shin, J Phys Chem B 112 (2008) 8476–8480.
[49] S. Lee, I.-S. Cho, J.H. Lee, D.H. Kim, D.W. Kim, J.Y. Kim, H. Shin, J.-K. Lee, H.S. Jung, N.-G. Park, K. Kim, M.J. Ko, K.S. Hong, Chem Mater 22 (2010) 1958–1965.
[50] T. Peng, K. Fan, D. Zhao, J. Chen, J Phys Chem B 114 (2010) 22346–22351.
[51] D. Zhao, T. Peng, L. Lu, P. Cai, P. Jiang, Z. Bian, J Phys Chem B 112 (2008) 8486–8494.